# Next-to-leading Order Photon+Jet Cross Section

Yair Mulian
University of Santiago de Compostela
In collaboration with N. Armesto

# Forward Jet Production

The basic setup: a large-x parton from the proton scatters off the small-x gluon distribution in the target nucleus. The large-x parton is most likely a quark.
We adopt the formalism of the LC outgoing state, using the CGC effective theory together with the hybrid factorization.

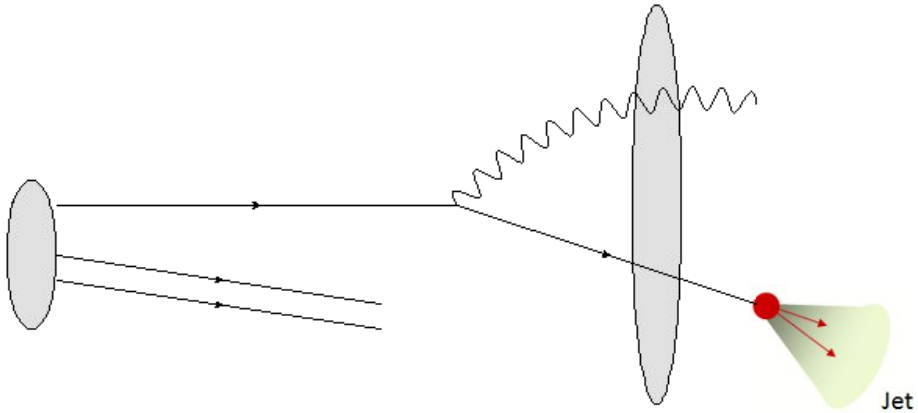


Quark emitting a photon in the presence of a shockwave.

# The Evolved Incoming State

The time evolution of the initial (bare) quark state is given by:

$$\left|q_\lambda^\alpha(q^+, \boldsymbol{q})\right\rangle_{in} \equiv U(0, -\infty)\, \left|q_\lambda^\alpha(q^+, \boldsymbol{q})\right\rangle$$

Where $U(t, t_0)$ denotes the unitary evolution operator, defined as

$$U(t, t_0) = T \exp\left\{-i \int_{t_0}^{t} dt_1\, V(t_1)\right\}$$

Where V denotes the interaction part of the QCD Hamiltonian.
Dyson's series:

$$U(t,t_0) = 1 - i\int_{t_0}^{t} dt_1 V(t_1) + (-i)^2 \int_{t_0}^{t} dt_1 \int_{t_0}^{t_1} dt_2 V(t_1)V(t_2) + \cdots$$
$$+ (-i)^n \int_{t_0}^{t} dt_1 \int_{t_0}^{t_1} dt_2 \cdots \int_{t_0}^{t_{n-1}} dt_n V(t_1)V(t_2)\cdots V(t_n) + \cdots.$$

At leading order:

$$|q\rangle_{in} \equiv \mathcal{Z}\,|q\rangle - |q_1\,\gamma\rangle\, \frac{\langle q_1\,\gamma|\, H\,|q\rangle}{E_{q_1\,\gamma} - E_q}$$

# The Outgoing State Formalism

The quark outgoing state is defined by:

$$\left|q_\lambda^\alpha(q^+,\boldsymbol{q})\right\rangle_{out} \equiv U(\infty,0)\,\hat{S}\,U(0,-\infty)\,\left|q_\lambda^\alpha(q^+,\boldsymbol{q})\right\rangle$$

hep-ph/0106240, A. Kovner and U. Wiedemann

This state encodes the information both on the ***time evolution*** and ***interaction with the target nucleus*** of the incoming quark state.

$$|q\rangle_{out} = V(q)\,|q\rangle + [2V(q_2) - V(q_1) - V(q)]\,\frac{1}{2}\,|q_1\rangle\,\frac{\langle q_1|\,H\,|q_2\,\gamma\rangle}{E_{q_2\,\gamma} - E_{q_1}}\,\frac{\langle q_2\,\gamma|\,H\,|q\rangle}{E_{q_2\,\gamma} - E_q}$$
$$- [V(q_1) - V(q)]\,|q_1\,\gamma\rangle\,\frac{\langle q_1\,\gamma|\,H\,|q\rangle}{E_{q_1\,\gamma} - E_q}.$$

The expectation values of operators are directly related to the outgoing state:

$$\left\langle\hat{\mathcal{O}}\right\rangle = \left\langle\,{}_{out}\langle q_\lambda^\alpha(q^+,\boldsymbol{w})|\,\hat{\mathcal{O}}\,|q_\lambda^\alpha(q^+,\boldsymbol{w})\rangle_{out}\,\right\rangle_{cgc}$$

# The LO Outgoing State

The outgoing state at leading order is given by

$$\left|q_\lambda^\alpha(q^+,\boldsymbol{w})\right\rangle_{out} \equiv U(0,\infty)\,\hat{S}\,U(0,-\infty)\left|q_\lambda^\alpha(q^+,\boldsymbol{w})\right\rangle = z\left|q_\lambda^\alpha(q^+,\boldsymbol{w})\right\rangle + \left|q_\lambda^\alpha(q^+,\boldsymbol{w})\right\rangle_{q\gamma}$$

The additional term reads:

$$\left|q_\lambda^\alpha(q^+,\boldsymbol{w})\right\rangle_{q\gamma}^{out} = -\int_{\boldsymbol{x},\boldsymbol{y}}\int_0^1 d\vartheta\,\frac{ig\sqrt{q^+}}{(2\pi)^2}\,\frac{\phi^{ij}_{\lambda_1\lambda}(\vartheta)}{\sqrt{2\vartheta}}\,\frac{\boldsymbol{R}^j}{\boldsymbol{R}^2}\,\delta^{(2)}(\boldsymbol{w}-(1-\vartheta)\boldsymbol{x}-\vartheta\boldsymbol{y})$$

$$\times\left[V^{\beta\alpha}(\boldsymbol{x})-V^{\beta\alpha}(\boldsymbol{w})\right]\left|q^\beta_{\lambda_1}((1-\vartheta)q^+,\boldsymbol{x})\,\gamma_i(\vartheta q^+,\boldsymbol{y})\right\rangle$$

Diagrammatically:

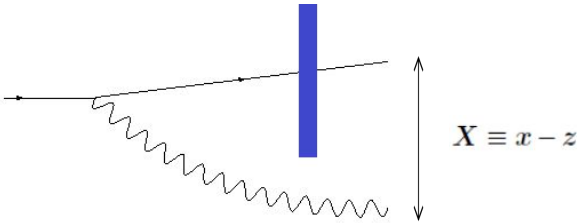


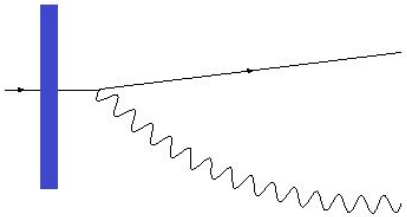

$$\vartheta \equiv k^+/q^+$$

$$U(\boldsymbol{x}) = \mathrm{T}\exp\left\{ig\int dx^+\,T^a A_a^-(x^+,\boldsymbol{x})\right\}$$

$$V(\boldsymbol{x}) = \mathrm{T}\exp\left\{ig\int dx^+\,t^a A_a^-(x^+,\boldsymbol{x})\right\}$$

Blue bar denotes a shockwave = interaction with the target.

# The LO Forward Photon+Jet Cross Section

From the production state we can pass easily to the quark-gluon dijet cross section:

$$\frac{d\sigma_{\rm LO}^{qA\to q\gamma+X}}{d^3k\,d^3p}\,(2\pi)\delta(k^+ + p^+ - q^+) \equiv \frac{1}{2N_c}\,{}^{out}_{q\gamma}\langle q^\alpha_\lambda(q^+,\boldsymbol{q})|\;\hat{\mathcal{N}}_q(p)\,\hat{\mathcal{N}}_\gamma(k)\;|q^\alpha_\lambda(q^+,\boldsymbol{q})\rangle^{out}_{q\gamma}$$

The following number density operators were introduced:

$$\hat{\mathcal{N}}_q(p) \equiv \frac{1}{(2\pi)^3}\,b^{\alpha\dagger}_\lambda(p)\,b^\alpha_\lambda(p) \qquad\qquad \hat{\mathcal{N}}_\gamma(k) = \frac{1}{(2\pi)^3}\,\alpha^\dagger_i(k)\,\alpha_i(k)$$

Then the result for the leading-order dijet cross section is given by:

$$\frac{d\sigma_{\rm LO}^{qA\to q\gamma+X}}{dk^+\,d^2\boldsymbol{k}\,dp^+\,d^2\boldsymbol{p}} = \frac{2\alpha_{e.m.}}{(2\pi)^6 q^+}\,\frac{1+(1-\vartheta)^2}{\vartheta}\,\delta(q^+-k^+-p^+)$$

$$\times\int_{\boldsymbol{x},\overline{\boldsymbol{x}},\boldsymbol{y},\overline{\boldsymbol{y}}}\frac{\boldsymbol{R}\cdot\overline{\boldsymbol{R}}}{\boldsymbol{R}^2\,\overline{\boldsymbol{R}}^2}\,{\rm e}^{-i\boldsymbol{p}\cdot(\boldsymbol{x}-\overline{\boldsymbol{x}})-i\boldsymbol{k}\cdot(\boldsymbol{y}-\overline{\boldsymbol{y}})}$$

$$\times\left[\mathcal{S}\left(\boldsymbol{w},\overline{\boldsymbol{w}}\right)-\mathcal{S}\left(\boldsymbol{x},\overline{\boldsymbol{w}}\right)-\mathcal{S}\left(\boldsymbol{w},\overline{\boldsymbol{x}}\right)+\mathcal{S}\left(\boldsymbol{x},\overline{\boldsymbol{x}}\right)\right]$$

hep-ph/0205037v1
By F. Gelis and J. J. Marian

An example for contribution which is included in the leading order result:

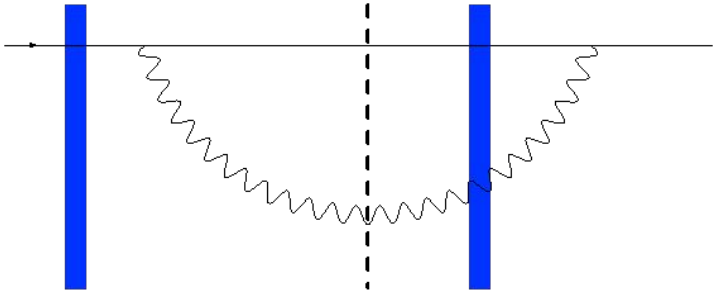

The dashed line, “the cut”, is the final state (the detector). The dipole is defined by:

$$\mathcal{S}\left(\overline{\boldsymbol{w}},\,\boldsymbol{w}\right) \equiv \frac{1}{N_c}\,\mathrm{tr}\left[V^{\dagger}(\overline{\boldsymbol{w}})\,V(\boldsymbol{w})\right]$$

From the partonic cross section we can find the quark channel contribution by convolution with the PDF:

$$\left.\frac{d\sigma_{\mathrm{LO}}^{pA\to q\gamma+X}}{d^3p\,d^3k}\right|_{q-channel} = \int dx_p\, q_f(x_p,\mu^2)\frac{d\sigma_{\mathrm{LO}}^{qA\to q\gamma+X}}{d^3p\,d^3k}$$

For measuring a photon+jet one has to convolute the result above with fragmentation/jet function:

$$\frac{d\sigma_{LO}^{pA\to jet+\gamma+X}}{d^3p\,d^3k} = \int\frac{dz_1}{z_1^3}\int\frac{dz_2}{z_2^3}\int dx_p\, q_f(x_p,\mu^2)\,\frac{d\sigma_{LO}^{pA\to q\gamma+X}}{d^3p\,d^3k}D_{jet/q}(z_1)\,J_{\gamma}(z_2)$$

# Motivations for NLO Calculations

The perturbative series for the cross section has the following structure:

$$\sigma_{photon+jet} = \boxed{\sigma(\alpha_{e.m.})} + \boxed{\sigma(\alpha_{e.m.}, \alpha_s)} + \sum_{n=2}^{\infty} \sigma(\alpha_{e.m.}, \alpha_s^n)$$

Leading Order

Next-to-leading Order (NLO)

The NLO term is necessary because:

a. NLO corrections considerably improve the accuracy of the theoretical results.

b. The NLO term contain built-in testable information on *saturation physics.*

c. Important step towards *all order resummation*.

# The Dijet+Photon Setup

Two possible configurations of 3 particles in the final state which are relevant for the cross section at order $\alpha_s \, \alpha_{e.m.}$ :

***a)*** ***Photon, quark and a gluon (quark channel)***,
***b)*** ***Quark, anti-quark and a photon (gluon channel)***.

The production of these configurations happen via two successive parton splittings (in the light-cone formalism, there are also 1->3 instantaneous vertices).

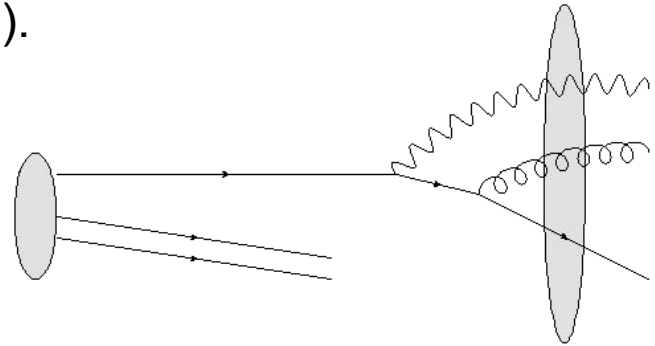

An example for a contribution with 3 particles in the final state

# Which Contributions Participate?

Direct and interference (regular and instantaneous emissions):

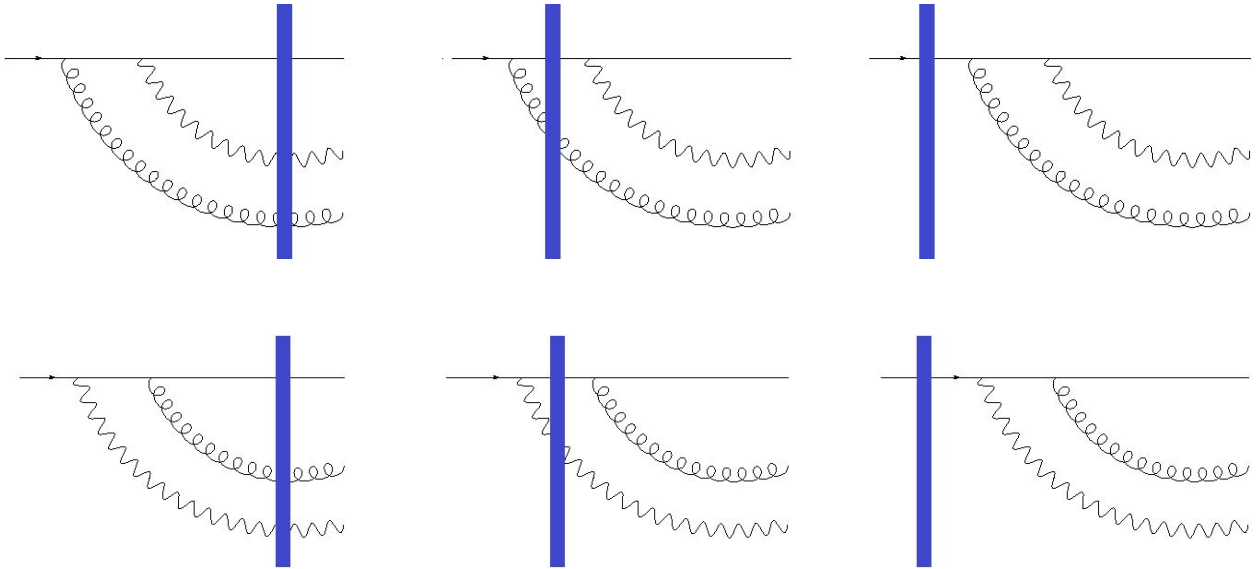

Some of the contributions already been computed at hep-ph/1802.01398v1 by T. Altinoluk, N. Armesto, A. Kovner, M. Lublinsky, E. Petreska. See also R. Boussarie, Marquet, P. Taels, hep-ph/1810.11273.

# From Photon+Dijet to "real" NLO Photon+Jet

The leading-order contribution to the photon+dijet cross section is:

$$\frac{d\sigma_{\rm LO}^{qA\to qg\gamma+X}}{d^3q_1\,d^3q_2\,d^3q_3}\,(2\pi)\delta(q_1+q_2+q_3-q^+) \equiv \frac{1}{2N_c}\;{}_{qg\gamma}\big\langle q_\lambda^\alpha(q^+,\boldsymbol{q})\big|\;\hat{\mathcal{N}}_q(q_1)\hat{\mathcal{N}}_g(q_2)\hat{\mathcal{N}}_\gamma(q_3)\;\big|q_\lambda^\alpha(q^+,\boldsymbol{q})\big\rangle_{qg\gamma}$$

The hadronic cross section is given by:

$$\frac{d\sigma^{pA\to q\gamma g+X}}{d^3q_\gamma\,d^3q_q\,d^3q_g} = \int dx_p\,q_f(x_p,\mu^2)\,\frac{d\sigma^{qA\to q\gamma g+X}}{d^3q_\gamma\,d^3q_q\,d^3q_g}$$

The real contribution for the NLO photon+jet cross section is related to photon+jet cross section by the integration over the unmeasured gluon:

$$\frac{d\sigma_{R\,nlo}^{qA\to q\gamma+X}}{d^3q_\gamma\,d^3q_q} = \int d^3q_g\,\frac{d\sigma^{qA\to q\gamma g+X}}{d^3q_\gamma\,d^3q_q\,d^3q_g}$$

hep-ph/2009.11930
by Y.M.
and E. Iancu

# The Real Cross Section

The quark quark anti-quark contribution reads:

$$\frac{d\sigma^{qA\to q\gamma g+X}}{dk_1^+\,d^2\boldsymbol{k}_1\,dk_2^+\,d^2\boldsymbol{k}_2\,dk_3^+\,d^2\boldsymbol{k}_3} = \frac{\alpha_s\,\alpha_{e.m.}\,C_F}{2(2\pi)^{10}(q^+)^2}\,\delta(q^+-k_1^+-k_2^+-k_3^+)$$

$$\times \int_{\overline{\boldsymbol{x}},\overline{\boldsymbol{z}},\overline{\boldsymbol{z}}',\boldsymbol{x},\boldsymbol{z},\boldsymbol{z}'} e^{-i\boldsymbol{k}_1\cdot(\boldsymbol{x}-\overline{\boldsymbol{x}})-i\boldsymbol{k}_2\cdot(\boldsymbol{z}-\overline{\boldsymbol{z}})-i\boldsymbol{k}_3\cdot(\boldsymbol{z}'-\overline{\boldsymbol{z}}')}\,\frac{\boldsymbol{R}^i\,\boldsymbol{Z}^j\,\overline{\boldsymbol{R}}^m\,\overline{\boldsymbol{Z}}^n}{\boldsymbol{Z}^2\,\overline{\boldsymbol{Z}}^2}$$

$$\times \Big[\mathcal{K}_0^{ijmn}(\boldsymbol{x},\,\boldsymbol{z},\,\boldsymbol{z}',\,\overline{\boldsymbol{x}},\,\overline{\boldsymbol{z}},\,\overline{\boldsymbol{z}}',\,\vartheta,\,\xi)\,\mathcal{W}_0\left(\boldsymbol{z},\,\boldsymbol{z}',\,\overline{\boldsymbol{z}},\,\overline{\boldsymbol{z}}'\right)$$

$$-\left(\boldsymbol{z},\,\boldsymbol{z}'\to\boldsymbol{y}\right)-\left(\overline{\boldsymbol{z}},\,\overline{\boldsymbol{z}}'\to\overline{\boldsymbol{y}}\right)+\left(\boldsymbol{z},\,\boldsymbol{z}'\to\boldsymbol{y}\;\&\;\overline{\boldsymbol{z}},\,\overline{\boldsymbol{z}}'\to\overline{\boldsymbol{y}}\right)\Big]$$

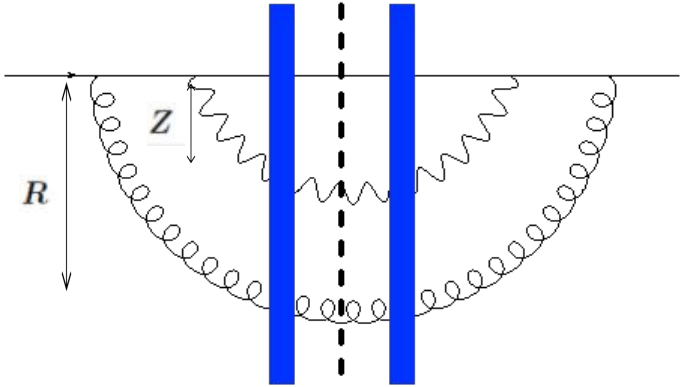


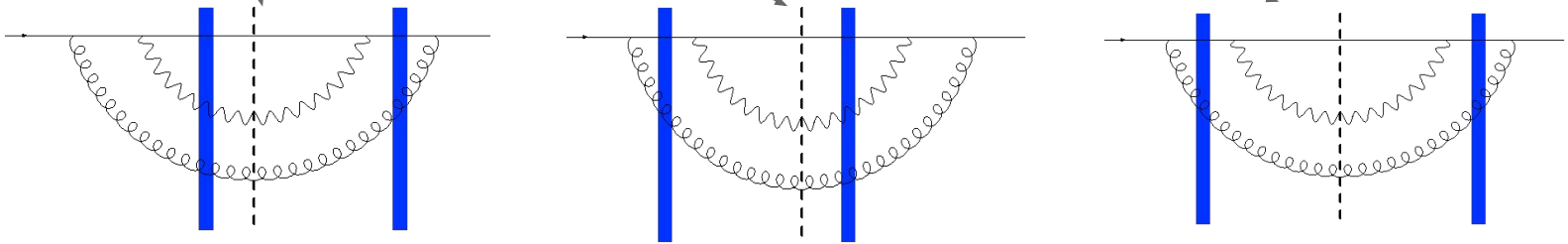

Similar structure to hep-ph/2009.11930.

# The Real Kernel

The kernel defined by:

$$\mathcal{K}_1^{imjn}(\boldsymbol{x},\boldsymbol{y},\boldsymbol{z},\overline{\boldsymbol{x}},\overline{\boldsymbol{y}},\overline{\boldsymbol{z}},\vartheta,\xi,Q) \equiv \Phi_{\lambda_1\lambda}^{lirm}(\boldsymbol{x},\boldsymbol{y},\boldsymbol{z},\vartheta,\xi)\,\Phi_{\lambda_1\lambda}^{ljrn\,*}(\overline{\boldsymbol{x}},\overline{\boldsymbol{y}},\overline{\boldsymbol{z}},\vartheta,\xi) \times \frac{\mathrm{K}_1\left(\bar{Q}D(\boldsymbol{x},\boldsymbol{y},\boldsymbol{z},\vartheta,\xi)\right)\,\mathrm{K}_1\left(\bar{Q}D(\overline{\boldsymbol{x}},\overline{\boldsymbol{y}},\overline{\boldsymbol{z}},\vartheta,\xi)\right)}{D(\boldsymbol{x},\boldsymbol{y},\boldsymbol{z},\vartheta,\xi)\,D(\overline{\boldsymbol{x}},\overline{\boldsymbol{y}},\overline{\boldsymbol{z}},\vartheta,\xi)}$$

With effective vertex, combining the regular and instantaneous emissions:

$$\Phi_{\lambda_1\lambda_2}^{ijmn}(\boldsymbol{x},\boldsymbol{y},\boldsymbol{z},\vartheta,\xi) \equiv \varphi_{\lambda_1\lambda}^{ij}(\vartheta)\,\tau_{\lambda\lambda_2}^{mn}(\xi,1-\vartheta-\xi) - \delta^{nj}\sqrt{\xi}(1-\vartheta)\left(\chi_{\lambda_1}^{\dagger}\sigma^i\sigma^m\chi_{\lambda_2}\right)\frac{\boldsymbol{Y}^2}{\boldsymbol{R}\cdot\boldsymbol{Y}}$$

And:

$$\vartheta = \frac{k_1^+}{q^+}, \qquad \xi = \frac{k_3^+}{q^+} \qquad D(\boldsymbol{x},\boldsymbol{y},\boldsymbol{z},\vartheta,\xi) \equiv \sqrt{\boldsymbol{R}^2 + \frac{\xi(1-\vartheta-\xi)}{\vartheta(1-\vartheta)^2}\boldsymbol{Y}^2}$$

# Recovering the JIMWLK Evolution

In the limit where the gluon become soft (eikonal emission vertex = no recoil of the emitter), the general NLO result has to reduce to one step in the real part of the production JIMWLK evolution of the LO photon+jet production cross section. We managed to show that this is indeed the case in our result.

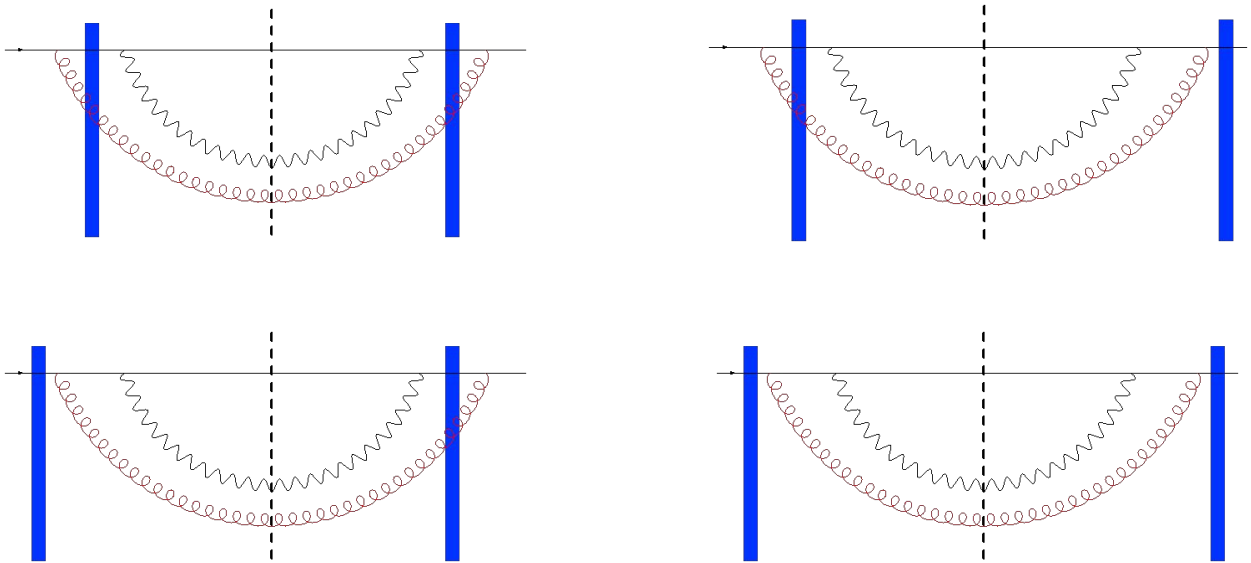

The four diagrams precisely reproduce the the BK evolution of the dipole $\mathcal{S}(w, \overline{w})$ of the leading order cross-section.

$$\frac{d\sigma^{qA\to q\gamma+X}_{\mathrm{NLO},1}}{dk_1^+\, d^2\boldsymbol{k}_1\, dk_3^+\, d^2\boldsymbol{k}_3} \simeq \frac{\alpha_{e.m.}}{(2\pi)^5}\,\frac{1+(1-\vartheta)^2}{2\vartheta q^+}\,\delta(q^+-k_1^+-k_3^+)$$

$$\times \int_{\overline{\boldsymbol{x}},\,\overline{\boldsymbol{z}}',\,\boldsymbol{x},\,\boldsymbol{z}'} e^{-i\boldsymbol{k}_1\cdot(\boldsymbol{x}-\overline{\boldsymbol{x}})-i\boldsymbol{k}_3\cdot(\boldsymbol{z}'-\overline{\boldsymbol{z}}')}\,\frac{(\boldsymbol{x}-\boldsymbol{z}')\cdot(\overline{\boldsymbol{x}}-\overline{\boldsymbol{z}}')}{(\boldsymbol{x}-\boldsymbol{z}')^2(\overline{\boldsymbol{x}}-\overline{\boldsymbol{z}}')^2}$$

→ LO result

$$\times \frac{\bar{\alpha}_s}{2\pi}\int_0^1\frac{d\xi}{\xi}\int_{\boldsymbol{z}}\frac{2(\boldsymbol{w}-\boldsymbol{z})\cdot(\overline{\boldsymbol{w}}-\boldsymbol{z})}{(\boldsymbol{w}-\boldsymbol{z})^2(\overline{\boldsymbol{w}}-\boldsymbol{z})^2}\left[\mathcal{S}(\boldsymbol{w},\overline{\boldsymbol{w}})-\mathcal{S}(\boldsymbol{w},\boldsymbol{z})\,\mathcal{S}(\boldsymbol{z},\overline{\boldsymbol{w}})\right]$$

→ BK evolution of $\mathcal{S}(w, \overline{w})$

Similarly, the following diagrams generate the evolutions of the dipole $\mathcal{S}(\boldsymbol{x}, \overline{\boldsymbol{x}})$:

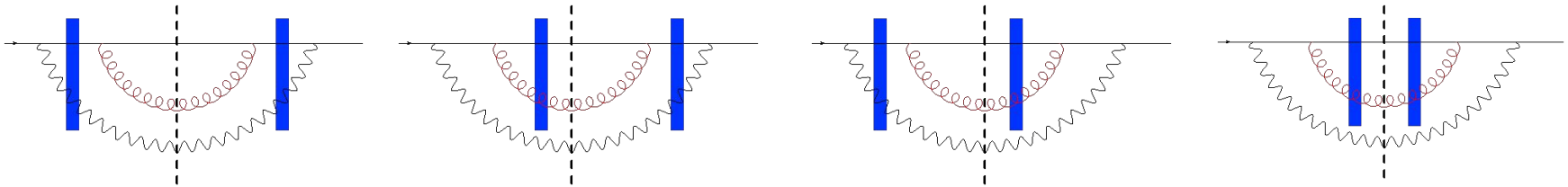

For the dipole $\mathcal{S}(\boldsymbol{w}, \overline{\boldsymbol{x}})$ :

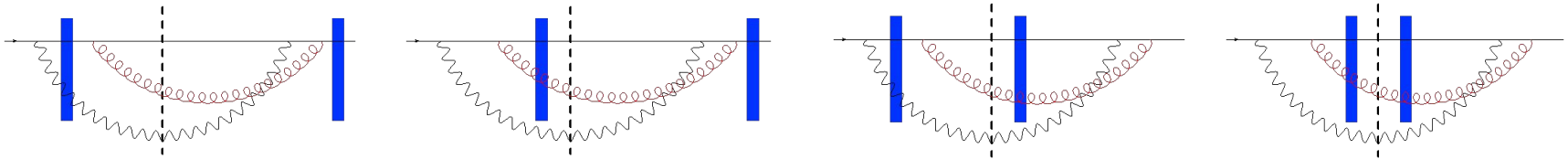

# Recovering the Real DGLAP Evolution

In the collinear limit, when the separation between partons become arbitrarily large, we recover the DGLAP evolution of the initial quark pdf and final quark jet function.

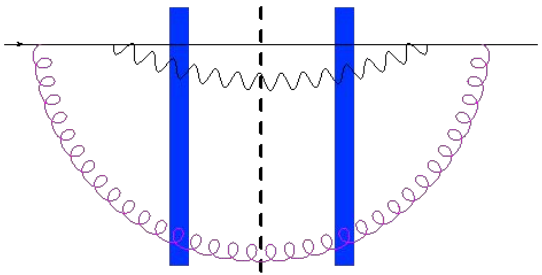

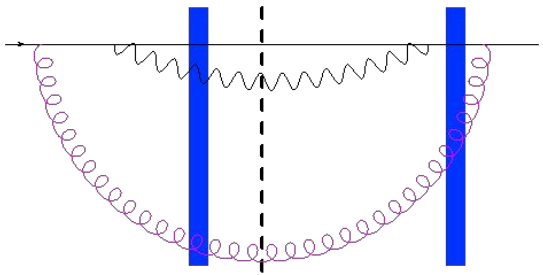

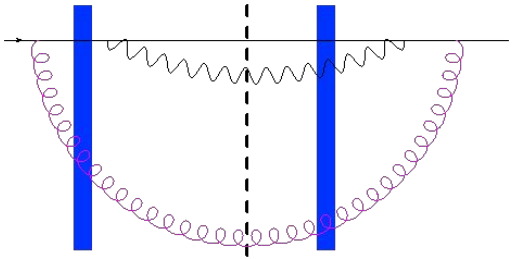

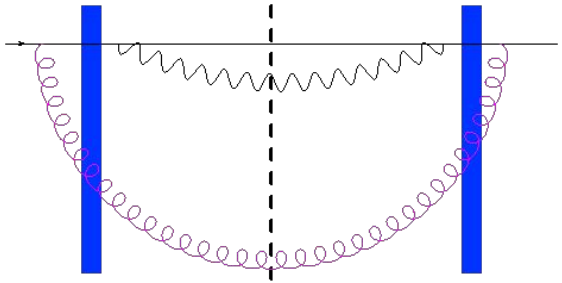

Combining the relevant four contributions:

$$\frac{d\sigma^{qA\to q\gamma+X}}{dp^+\,d^2\boldsymbol{p}\,dk^+\,d^2\boldsymbol{k}} \simeq \frac{4\alpha_{e.m.}}{(2\pi)^6(q^+)^2(1-\xi)}\,P_{q\to\gamma}\Big(\frac{x_2}{x_1+x_2}\Big)$$
$$\times \int_{\overline{\boldsymbol{x}},\,\overline{\boldsymbol{z}}',\,\boldsymbol{x},\,\boldsymbol{z}'} e^{-i\boldsymbol{p}\cdot(\boldsymbol{x}-\overline{\boldsymbol{x}})-i\boldsymbol{k}\cdot(\boldsymbol{z}'-\overline{\boldsymbol{z}}')}\,\frac{(\boldsymbol{x}-\boldsymbol{z}')\cdot(\overline{\boldsymbol{x}}-\overline{\boldsymbol{z}}')}{(\boldsymbol{x}-\boldsymbol{z}')^2(\overline{\boldsymbol{x}}-\overline{\boldsymbol{z}}')^2}$$
$$\times \Big[\mathcal{S}\,(\boldsymbol{x},\,\overline{\boldsymbol{x}}) - \mathcal{S}\,(\boldsymbol{x},\,\overline{\boldsymbol{w}}) - \mathcal{S}\,(\boldsymbol{w},\,\overline{\boldsymbol{x}}) + \mathcal{S}\,(\boldsymbol{w},\,\overline{\boldsymbol{w}})\Big]$$
$$\times \frac{4\alpha_s C_F}{(2\pi)^2}\,P_{q\to g}(\xi)\int_{\boldsymbol{z}} \frac{(\boldsymbol{y}-\boldsymbol{z})\cdot(\overline{\boldsymbol{y}}-\boldsymbol{z})}{(\boldsymbol{y}-\boldsymbol{z})^2(\overline{\boldsymbol{y}}-\boldsymbol{z})^2}\,.$$

The result above is precisely the result of one “real” step in the DGLAP evolution of the quark distribution inside the proton:

$$x\Delta q_f(x,\mu^2) \equiv \frac{\alpha_s C_F}{\pi}\int_0^{1-x} d\xi\,\frac{x}{1-\xi}\,q_f\Big(\frac{x}{1-\xi},\mu^2\Big)P_{q\to g}(\xi)\,\ln\frac{\mu^2}{\Lambda^2}$$

# The Virtual Contributions

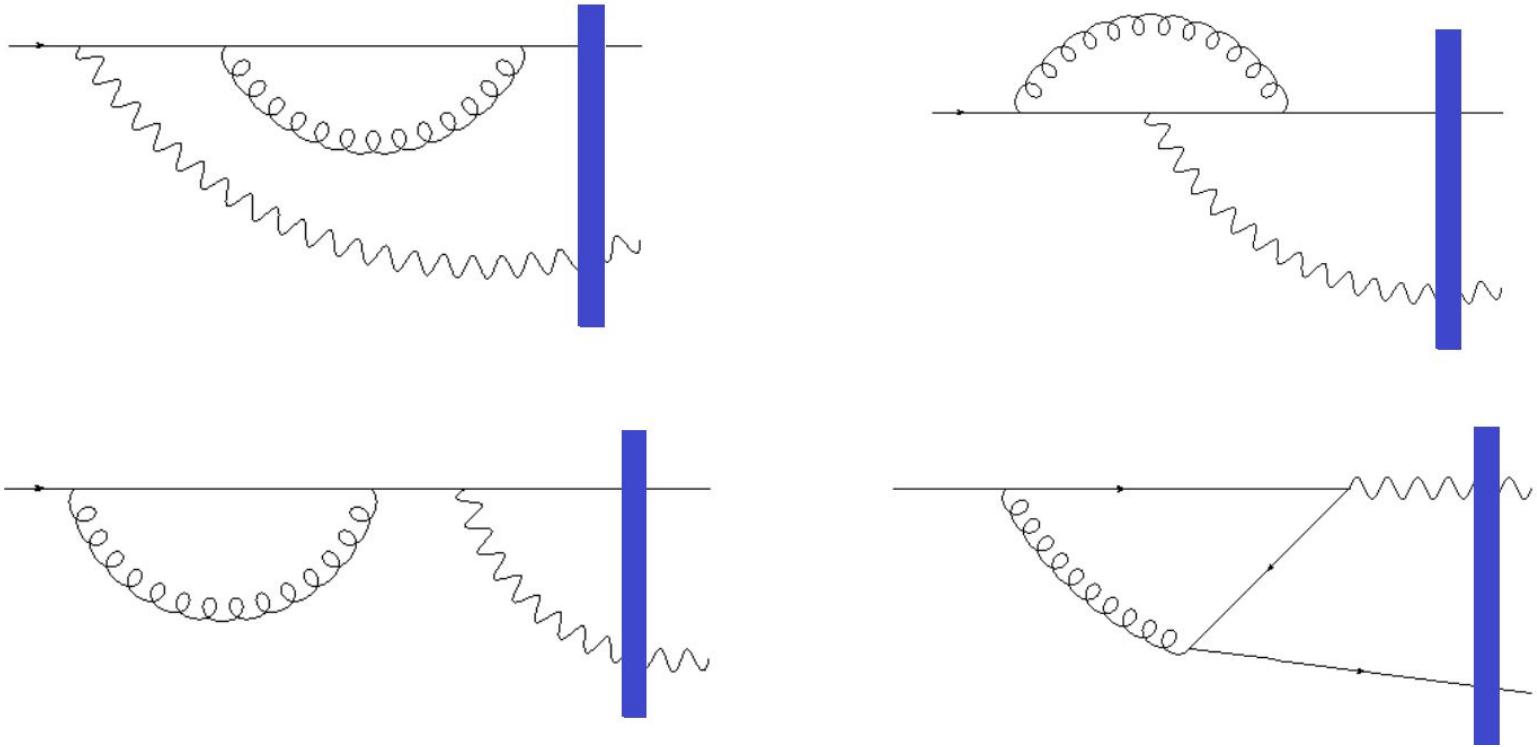

# The Generic Structure with Shockwave at the End

The diagrams in which the shockwave is at the end contain both UV and soft divergences.

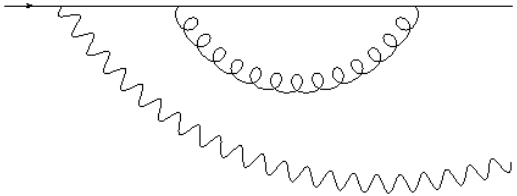

For the above contribution, after using dimreg and sharp cutoff regularizations:

$$
\begin{aligned}
|\psi_{\lambda}^{\alpha}\rangle_{q\gamma}^{1} &= \int_0^1 d\vartheta \int d^2\widetilde{\boldsymbol{k}}\, \frac{ee_f g^2\, \phi_{\lambda_1\lambda}^{ij}(\vartheta)\, \widetilde{\boldsymbol{k}}^j\, \sqrt{q^+}}{8(2\pi)^5 \sqrt{2(1-\vartheta)}\, \widetilde{\boldsymbol{k}}^2} \left( \left[ 3 + 4\ln\left(\frac{\Lambda}{\vartheta q^+}\right)\right] \right. \\
&\times \left[ -\frac{2}{\epsilon} + \ln\left(\frac{\widetilde{\boldsymbol{k}}^2}{\mu_{\overline{MS}}^2}\right)\right] + 2\ln^2\left(\frac{\Lambda}{\vartheta(1-\vartheta)q^+}\right) - 7 + \frac{2\pi^2}{3} - 2\ln^2(1-\vartheta) - 3\ln(1-\vartheta) \Big) \\
&\times \left| q_{\lambda_1}^{\alpha}(\vartheta q^+,\, \vartheta\boldsymbol{q} - \widetilde{\boldsymbol{k}})\, \gamma_i((1-\vartheta)q^+,\, (1-\vartheta)\boldsymbol{q} + \widetilde{\boldsymbol{k}}) \right\rangle
\end{aligned}
$$

Two types of IR logs are involved: $\ln\left(\frac{\Lambda}{q^+}\right)\ln\left(\frac{\widetilde{\mathrm{k}}^2}{\mu_{\overline{MS}}^2}\right)$ and $\ln^2\left(\frac{\Lambda}{\vartheta(1-\vartheta)q^+}\right)$

Both IR logs are canceled when combining the various contributions.

# “Shock in the middle” Diagrams

Additional class of virtual diagrams involve the shockwave on an intermediate state:

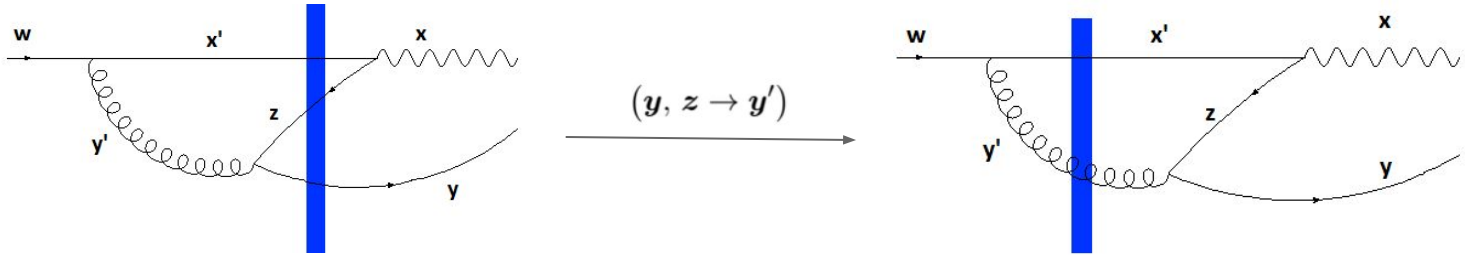


The corresponding cross section can be written as:

$$\frac{d\sigma^{qA\to q\gamma+X}}{dk_1^+\,d^2\boldsymbol{k}_1\,dk_2^+\,d^2\boldsymbol{k}_2} = \frac{\alpha_s\,\alpha_{e.m.}\,C_F\,N_f}{2(2\pi)^6 q^+}\,\delta(q^+ - k_1^+ - k_2^+)$$
$$\times \int_{\overline{\boldsymbol{x}},\overline{\boldsymbol{y}},\boldsymbol{x}',\boldsymbol{y},\boldsymbol{z}} e^{-i\boldsymbol{k}_1\cdot(\boldsymbol{x}-\overline{\boldsymbol{x}})-i\boldsymbol{k}_2\cdot(\boldsymbol{y}-\overline{\boldsymbol{y}})}\,\frac{\widetilde{\boldsymbol{R}}^i\,(\boldsymbol{X}')^j\,\boldsymbol{Y}^m\,\overline{\boldsymbol{R}}^n}{\widetilde{\boldsymbol{R}}^2\,(\boldsymbol{X}')^2\,\boldsymbol{Y}^2}$$
$$\times \left[\mathbb{K}_0^{ijmn}(\boldsymbol{x}',\boldsymbol{y},\boldsymbol{z},\overline{\boldsymbol{x}},\overline{\boldsymbol{y}},\vartheta)\,\mathbb{W}_0\,(\boldsymbol{x}',\boldsymbol{y},\boldsymbol{z},\overline{\boldsymbol{y}}) - \frac{1}{2}(\boldsymbol{y},\boldsymbol{z}\to\boldsymbol{y}')\right]$$

In order to tackle these diagrams one has to revise the current understanding of normalization. “On the exact solution for the Schrodinger equation” to be published soon.

# What's Next?

***Including the gluon channel***: the contributions which involve incoming gluon are necessary in order to fully absorb all the various divergences in a consistent manner.

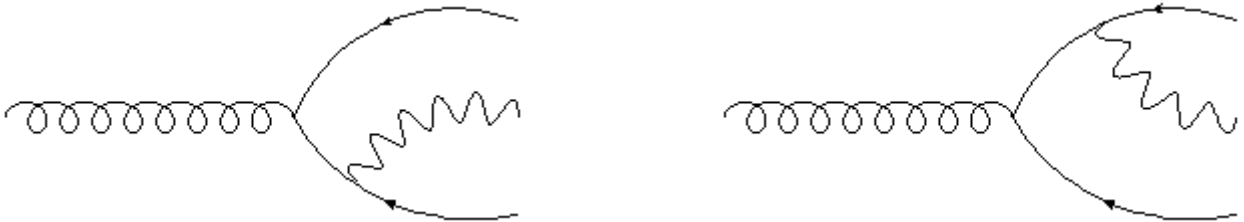

Needed in order to extend the rapidity domain of the calculation and to recover full DGLAP.

# Summary

1) The full results (real and virtual) for the NLO cross section for photon+jet production of an incoming quark are on the way.

2) Short-distance poles has been shown to cancel between pairs of diagrams. The IR logs are canceled when combining together the virtual diagrams.

3) Match has been established between the eikonal (collinear) limit of the result and the JIMWLK (DGLAP) evolution of the LO cross section for photon+jet production.